Morphological and Scattering Studies of Binary Mixtures of Block Copolymers: Cosurfactant Effects Observed in the Parameter Space of Temperature, Blend Composition, and Molecular Weight Ratio

François Court,[†,‡,§] Daisuke Yamaguchi,[†,||] and Takeji Hashimoto*[,†,||]

Department of Polymer Chemistry, Graduate School of Engineering, Kyoto University, Katsura, Nishikyo-ku, Kyoto 615-8510, Japan, Laboratoire de Physico-Chimie Structurale et Macromoléculaire, ESPCI, 10 rue Vauquelin, 75005 Paris, France, and Advanced Science Research Center, Japan Atomic Energy Agency, Tokai-mura, Ibaraki Prefecture, 319-1195, Japan

Received January 15, 2008; Revised Manuscript Received March 27, 2008

ABSTRACT: Thermoreversible order-order transitions or "order−distorted order" transitions (defined "OOT" for simplicity) between various morphologies occurring on binary mixtures of diblock copolymers were investigated by using small-angle X-ray scattering. The mixtures were composed of a long asymmetric polystyrene-*block*-polyisoprene (SI) having a spherical morphology and a short symmetric SI, which are hereafter denoted as *as* and s_3, respectively. The symmetric diblock, s_3, is short enough to be in a disordered state at room temperature. Upon raising temperature from ambient temperature toward order−disorder or "distorted order-disorder" transition temperature, a unique re-entrant bicontinuous-cylinder- bicontinuous OOT was observed for $as/s_3 = 85/15$ and 82/18 (w/w). Other types of OOT, such as cylinder-sphere and lamella-bicontinuous, were observed on the as/s_3 mixtures of different compositions. These OOTs were characterized by monitoring the evolution of the inverse peak scattered intensity, the square of the half-width at half-maximum of the peak, and the characteristic period of the microdomains, as a function of temperature, T. The complex morphological behaviors observed here can be understood on the basis of two key features of the binary blends: the cosurfactant effect and the possibility for the chemical junctions of the shorter diblock to migrate away from the interface as segregation power decreases. As a summary of this series of studies, a three-dimensional phase diagram was constructed in the parameter space of overall volume fraction of PS block in the mixture, the ratio of the degree of polymerization of *as* to that of s_3 and T. Such a phase diagram illustrates that the *cosurfactant effect* opens perspectives in tailoring morphologies of self-assembled, nanostructured materials.

I. Introduction

In this series of works, we explore the morphological behavior of binary mixtures of polystyrene (PS)-*block*-polyisoprene (PI) diblock copolymer (SI) composed of a long asymmetric SI denoted as *as* and a short symmetric SI denoted as s_i ($i = 1$, 2, or 3), based on the key concept of "*cosurfactant effect*".[1−3] The *cosurfactant effect* controls the interface curvature and the size of microdomains when chemical junction points of two block copolymers having considerably different block lengths share a common interface.[4−12] In this paper, we aim to complete the phase diagram of as/s_i ($i = 1-3$) in the parameter space of T, ϕ_{PS}, and r by combining the new results obtained in this work and all the results obtained so far from this series of works. These parameters T, r, and ϕ_{PS} will be defined below.

The *cosurfactant effect* on the as/s_i system was investigated at an ambient temperature[1,2] as well as at varying temperatures for a fixed $r = 4.4$ and a limited number of blend compositions (see Figure 1).[3] The works elucidated the following features: (i) The morphology and phase diagram of the as/s_i system, which was constructed at an ambient temperature and in the parameter space of r, which is defined as the ratio of degree of polymerization (DP) of *as* (hereafter, denoted as N_{as}) to that of s_i (N_{si}), $r \equiv N_{as}/N_{si}$, and overall volume fraction of PS block in the mixture, ϕ_{PS}, revealed that the stability limit of each morphology for as/s_i system is shifted with respect to ϕ_{PS} from that of the neat block copolymers.[1] Figure 1 demonstrates this effect only for as/s_3. That is, the stability range of the lamellar phase is enlarged as compared with that of neat block copolymer system, as seen by a shift of the lower bound of its stability limit to a lower ϕ_{PS}. (ii) The above feature (i) is enhanced as r increases (see Figure 11 of ref 1). (iii) The mixtures having lamellar morphology at the ambient temperature ($as/s_3 = 45/55$ and 75/25 mixtures) transformed into a "distorted bicontinuous" morphology with increasing temperature (T).[3] Namely, at low Ts the lamellar phase is stabilized by the *cosurfactant effect*, whereas at high Ts the "distorted bicontinuous" phase is stabilized (see Figure 1). Such a complex morphological behavior proves that the *cosurfactant effect* plays a crucial role on morphology as a consequence of the competing long-range interactions of the component block chains in microdomain space.[10−12]

It is worth while to remark on the "distorted bicontinuous" morphology at this point. As described in detail in the previous work,[3] the "distorted bicontinuous" morphology belongs to a microphase-separated one having a well-defined interface.[3] Though it has a large distortion in its long-range order, it is definitely different from the disordered structure, predicted by Fredrickson and Helfand,[13] above the weakly first order phase transition of the so-called order−disorder transition (ODT). The fluctuation-induced disordered structure was visualized by the computer simulation[14] and by transmission electron micrographs[15] taken on the samples rapidly quenched from the disordered phase close to the ODT temperature (T_{ODT}) to ice−water (0 °C) well below the glass transition temperature and denoted by the "D_F structure".[14,15] Although in the context of the current theory,[13,16] such a microdomain structure without a long-range order and a clear symmetry is defined to be a

* To whom correspondence should be addressed. E-mail: hashimoto.takeji@jaea.go.jp
† Department of Polymer Chemistry, Graduate School of Engineering, Kyoto University.
‡ Laboratoire de Physico-Chimie Structurale et Macromoléculaire, ESPCI.
§ Present address: COATEX, 35 rue Ampère, 69730 Genay, France.
|| Advanced Science Research Center, Japan Atomic Energy Agency.

10.1021/ma800102a CCC: $40.75 © 2008 American Chemical Society
Published on Web 06/04/2008

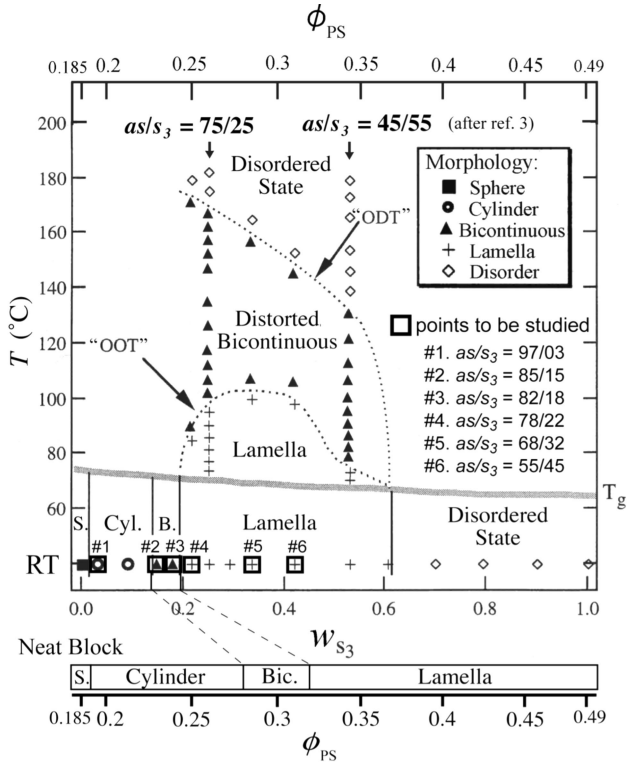

Figure 1. Phase diagram of as/s_3 mixtures in the parameter space of temperature (T) and weight fraction of s_3 (w_{s_3}) or volume fraction of PS (ϕ_{PS}) in the mixtures. The data of as/s_3 =45/55 and 75/25 were obtained from ref 3 of this series of papers.[1–3] The temperature dependence of other mixtures, marked by the symbols and numbered 1 to 6, are to be explored in this study. See the meaning of quotation marks attached to ODT and OOT in the text.

structure in the disordered state, we would like to emphasize that the "distorted bicontinuous" morphology is quite different from the morphology in the disordered phase having no microdomains but only concentration fluctuations that can be predicted by the RPA theory.[13,16] Hence, it is different from the D_F structure which reflects a large amplitude of dynamical concentration fluctuations in the disorder phase close to T_{ODT}.

In this study, we will further investigate the temperature-induced thermo-reversible order-order transition (OOT) occurring in the as/s_3 mixtures, including not only lamellar-bicontinuous "OOT" [in as/s_3 = 55/45 (no. 6), 68/32 (no. 5) and 78/22 (no. 4)] but also bicontinuous-cylinder OOT [in as/s_3 = 82/18 (no. 3) and 85/15 (no. 2)] and sphere-cylinder OOT [in as/s_3 = 97/03 (no. 1)] in Figure 1. The mixtures to be investigated in this work are distinguished from the others obtained in the previous work[3] in Figure 1 by the symbols (+, ▲, and ○) encompassed with the thick squares and the numbers (no. 1 to no. 6). The term lamellar-bicontinuous "OOT" used here follows the one previously defined.[3] However in a more rigorous sense, we should replace lamellar-bicontinuous by lamellar-distorted bicontinuous and "OOT" by "order−distorted order" transition ("OdOT").

We would like to add a remark on the term "ODT" with quotation mark in Figure 1. This "ODT"[3] denotes the transition between distorted bicontinuous phase and the disorder phase as described above, and hence may be called "distorted order−disorder transition" (dODT). The dODT is different from the ODT well established by earlier theories[13,16–18] and experiments.[19–23] The scattering from the distorted bicontinuous phase at higher temperatures close to "ODT" (or "dODT") is similar to that from the disordered bicontinuous structure (or sponge-like structure) in the spinodally phase-separated blends,[19,24–29]

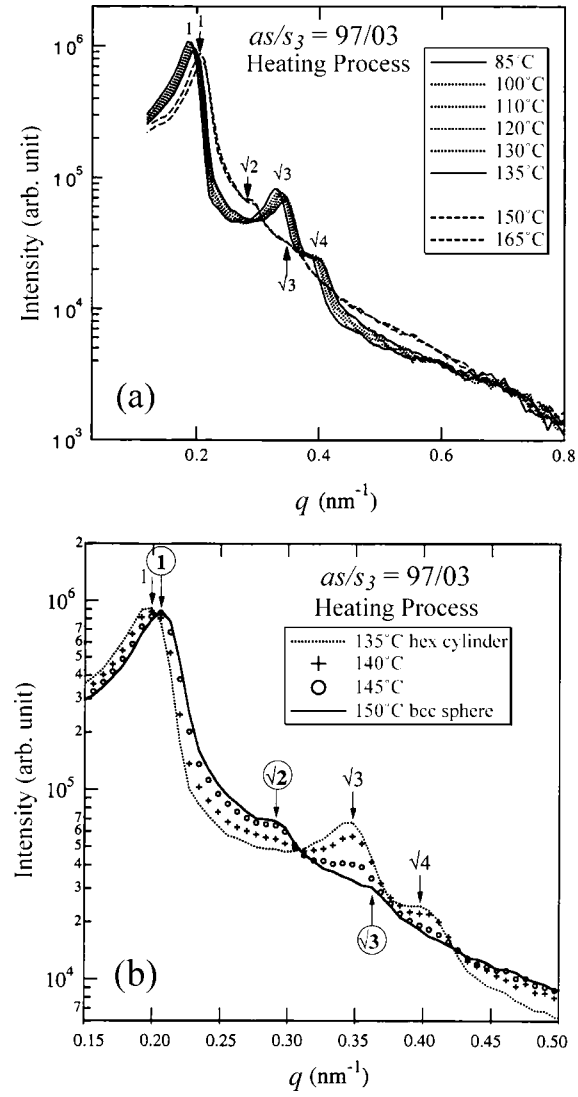

Figure 2. SAXS profiles of as/s_3 = 97/03 measured at different temperatures on the heating process: (a) the temperature range, in which the mixture shows hex cylinder (from 85 to 135 °C) and bcc sphere (150 and 165 °C), respectively; (b) the temperature range of OOT from hex cylinder to bcc sphere. The profiles measured at 140 and 145 °C indicate the coexistence of hex cylinder and bcc sphere.

though the scattering from the former at low temperatures is much sharper than the scattering from the latter. In this sense "ODT" (or "dODT") may be coined "disorder (with microdomains) to disorder (with concentration fluctuations) transition" ("$D_{md}D_{cf}T$"). Here it is important to note that the disordered (or distorted) bicontinuous structure is the microphase-separated structure having an interface between the coexisting microdomain structures, hence having more order than the disordered phase described by RPA theory.[13,16] It is quite natural that "dODT" or "$D_{md}D_{cf}T$" is not accompanied by the discontinuous change in I_m^{-1} vs T^{-1} and σ_q^2 vs T^{-1} as found in our experimental results shown in Figures 2 and 3 in ref 3, because the transition is not first order.

In the literature, several investigations have been conducted on the temperature-induced OOT of neat diblock copolymers[30–36] The first thermo-reversible OOT was identified for a neat diblock copolymer between a body-centered-cubic (BCC) sphere and a hexagonal cylinder by Sakurai et al.[30] Later on, various thermo-reversible OOT were found in the vicinity of ODT, and in this context, the bicontinuous gyroid morphology was identified in the phase diagram of neat diblock copolymer.[31–33] Furthermore, very recently the temperature-induced

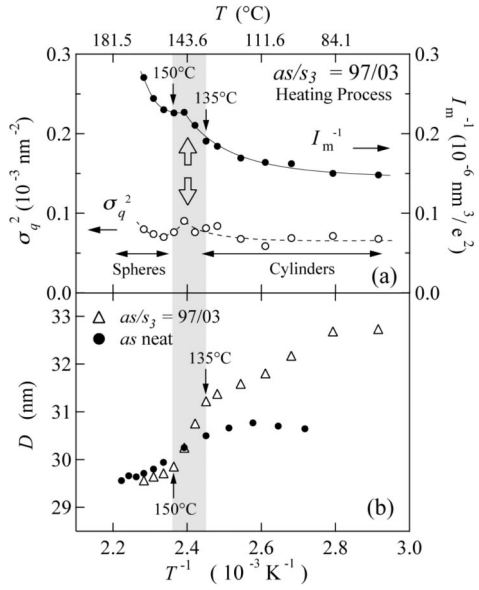

Figure 3. (a) Temperature dependence of the characteristics of the first-order scattering peak, I_m^{-1} and σ_q^2, for as/s_3 = 97/03 mixture; (b) comparison of the temperature dependence of D, the Bragg spacing, of as/s_3 = 97/03 mixture with that of *as* neat copolymer. A shaded region represents the temperature range where OOT between hex cylinder and bcc sphere occurs.

OOT including *Fddd* orthorhombic network structure has been predicted[34] and observed in a neat diblock copolymer,[35] indicating that this research topic is active.

On the other hand, as for the thermo-reversible OOT of the binary mixture of diblock copolymers, some important experimental findings have been reported on the gyroid morphology[36,37] and on a general phase diagram in the parameter space of temperature and composition for the binary mixtures of poly(ethylene)-*block*- poly(ethylethylene).[38] However, there are very few experimental studies, which focus on the *cosurfactant effect*.[4]

II. Experimental Methods

II.1. Sample Preparation. SI diblock copolymers were prepared by sequential living anionic polymerization as described in the previous publication[1]. Table 1 summarizes the characteristics of the synthesized diblocks, *as* and s_3. The film specimens of *as* and s_3 as well as those of the mixtures of as/s_3 = 55/45, 68/32, 78/22, 82/18, 85/15, and 97/03 (w/w) were prepared at room temperature by the solution-cast method as described elsewhere.[1–3] The film specimens were further dried at 80 °C under vacuum until constant weights were attained. The film specimens thus obtained were annealed at 180 °C for several hours to eliminate the bubbles which might be generated in the specimens during the residual-solvent evaporation process at 80 °C. The film specimens were then employed for the *in situ* temperature dependent small-angle X-ray scattering (SAXS) measurements. During the annealing process and SAXS measurements, the specimens were always placed under vacuum to reduce thermal degradation as much as possible.

II.2. Small Angle X-ray Scattering. The microdomain structures were investigated by SAXS using a rotating anode X-ray generator operated at 50 kV and 200 mA.[39–41] The SAXS profiles were corrected for the air scattering, the absorption, and the slit height and slit width smearing effects.[39–44] The absolute SAXS intensity was determined by the nickel foil method.[45] The intensity profiles are represented as a function of magnitude of scattering vector, q, which is related to the scattering angle, θ, by

$$q = (4\pi/\lambda)\sin(\theta/2) \quad (1)$$

The thermal protocol employed in the SAXS experiments was as follows. The first series of measurements at each temperature was conducted during the cooling process starting from the highest temperature (180 °C), which was followed by the second series of measurements on the heating process from low temperature to high temperature. These two series of measurements permitted to confirm if the specimen was close to the equilibrium state at each temperature. Each SAXS profile was recorded for 1 h. When temperature was changed from one to another, it took 15 min. for the specimen to reach the set temperature. A 45 min additional waiting period was set before launching the SAXS measurement.

III. Results

III.1. Temperature Dependence of Neat Copolymers, *as* and s_3. The scattering profiles of neat *as* copolymer were measured at different temperatures, ranging from ambient temperature to 180 °C (although the scattering data itself are not shown in this paper). Up to 180 °C, the diblock copolymer *as* formed spherical microdomains of PS on the BCC lattice in the PI matrix. When this copolymer was heated more than 1 h at 180 °C, it was degraded and this degradation prevented the precise determination of ODT temperature (T_{ODT}) of this copolymer. The temperature dependence of s_3 copolymer (designated as OSI-1) had been previously investigated in detail by Sakamoto and Hashimoto.[46] This copolymer was in the disordered state over the entire temperature range investigated.

III.2. OOT between Hex Cylinder and BCC Sphere (C−S OOT). *III.2.1. Temperature Dependence of as/s_3 = 97/03 (no. 1).* The measured profiles at different temperatures between 85 and 165 °C are shown in Figure 2a. Between 85 and 135 °C, three peaks are observed at the relative peak positions of $1:\sqrt{3}:\sqrt{4}$, which are characteristics of the hexagonal cylinder morphology (hex cylinder). From 150 to 170 °C the profiles also present three peaks (though the third one is very broad or appears as a shoulder), but the relative positions of those peaks located at $1:\sqrt{2}:\sqrt{3}$, indicative of the body-centered cubic spheres (bcc sphere). Thus, the mixture as/s_3=97/03 undergoes an OOT between hex cylinder and bcc sphere (hereafter designated as C−S OOT), and its OOT temperature (T_{OOT}) is located somewhere between 135 and 150 °C.

The scattering profiles measured in the intermediate temperature region of C−S OOT, namely, at 140 and 145 °C, are shown in Figure 2b (focused on a narrow q range between 0.15 nm^{-1} and 0.5nm^{-1}). For the sake of comparison, the profiles measured at 135 and 150 °C, are also shown in Figure 2b. The three higher order peaks located at $q/q_m = \sqrt{2}$, $\sqrt{3}$, and $\sqrt{4}$ are distinct in the profiles measured at 140 and 145 °C, suggesting that the hex-cylinder and bcc-sphere morphologies are coexisting in this temperature range. Here q_m is the q value at the first order peak.

III.2.2. Comparison between as/s_3 = 97/03 and Neat as. The temperature dependence of the characteristic parameters of the first-order peak, i.e., I_m^{-1} and σ_q^2, of as/s_3 = 97/03 are shown in Figure 3a. The C−S OOT is reflected in the small discontinuous drop (marked by a thick open arrow) on the curve I_m^{-1} vs T^{-1}.

Figure 3b compares the Bragg spacing D of the microdomain structure between as/s_3=97/03 and neat *as* copolymer as function of T^{-1}. In this figure we can discern that above 150 °C, the spherical microdomain structure for the as/s_3 = 97/03 mixture and the neat *as* copolymer have almost identical dimensions. Consequently, the effect of the 3 wt % of the short diblock s_3 on the microdomain structure seems completely negligible in this temperature region. Contrarily, below 135 °C the role of only the 3 wt % of short diblock s_3 on D becomes remarkable. In this temperature range, the as/s_3=97/03 has hex cylinder as a consequence of C−S OOT, though neat *as* remains bcc sphere. Consequently, the temperature dependence of D of as/s_3 = 97/03 deviates from that of *as* neat copolymer. The

Table 1. Characteristics of the SI Diblocks

code	$\bar{M}_n \times 10^{-3}$ [a]	HI [b]	$\bar{M}_{n,PS} - \bar{M}_{n,PI} \times 10^{-3}$ [c]	$N_{PS} - N_{PI}$ [d]	N [e]	w_{PS} [f]	f_{PS} [g]
as	47.0	1.03	9.6−37.4	92−550	642	0.205	0.185
s_3	12.1	1.03	6.3−5.8	61−85	146	0.52	0.49

[a] $\bar{M}_n$: number average molecular weight determined by size exclusion chromatography (SEC). [b] $HI = \bar{M}_w/\bar{M}_n$: heterogeneity index for molecular weight distribution. [c] $\bar{M}_{n,k}$: number average molecular weight of the kth block (k = PS or PI). [d] N_k: number average degree of polymerization of the kth block (k = PS or PI). [e] N: total number average degree of polymerization of the diblock: $N = N_{PS} + N_{PI}$ [f] w_{PS}: polystyrene weight fraction. [g] f_{PS}: volume fraction of the PS block calculated from $f_{PS} = (w_{PS}/\rho_{PS})/(w_{PS}/\rho_{PS} + (1 - w_{PS})/\rho_{PI})$ by using the following densities for the PS and PI blocks, $\rho_{PS} = 1.0514$ g·cm^{-3} and $\rho_{PI} = 0.925$ g·cm^{-3}.

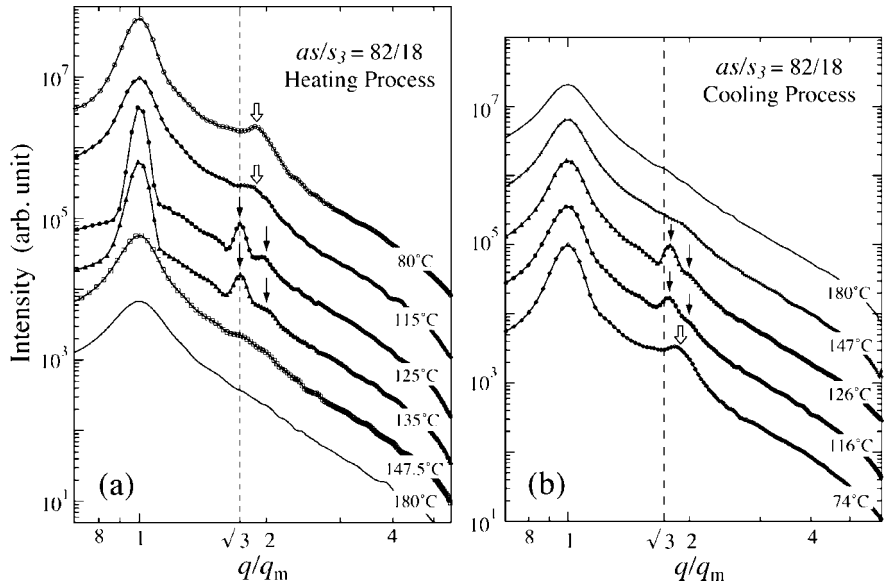

Figure 4. SAXS profiles of $as/s_3 = 82/18$ mixture measured at different temperatures: (a) under the heating process from 80 °C; (b) under the cooling process from 180 °C. In both part a and b, the scattering curves are vertically shifted by factor 5. The horizontal axis is not q itself but normalized by q_m, where q_m denotes the q value at the first-order scattering peak.

presence of 3% of short diblocks influences the microdomain morphology in such a way that the cylindrical packing becomes more favorable than the spherical one at low temperatures.

III.3. Transition between Bicontinuous and Hex Cylinder. At the ambient temperature the stability range of the bicontinuous morphology for as/s_3 appeared to be very narrow (see Figure 1). The stability range in terms of the overall PS volume fraction, hereafter designated as $(\phi_{PS,Bic})_{as/s_3}$, is given by $0.225 \leq (\phi_{PS,Bic})_{as/s_3} < 0.24$.[1] The two samples investigated here, $as/s_3 = 85/15$ (no. 2) and $as/s_3 = 82/18$ (no. 3) having very similar morphology, exhibited the bicontinuous morphology at ambient temperature.[1] In this work, we compare the morphological change in these two mixtures with temperature.

III.3.1. Observation with Polarized Optical Microscopy. Before presenting the SAXS results, the optical properties of the specimens as a function of temperature are briefly summarized here. As for the protocol, the specimens were annealed for 1 h at different temperatures prior to the observation at each temperature. The following results were obtained: (i) At ambient temperature, both $as/s_3 = 82/18$ (no. 3) and $as/s_3 = 85/15$ specimens (no. 2) dried at 80 °C, whose morphologies have proven to be a bicontinuous morphology[1], showed no birefringence. (ii) On heating from ambient temperature, the $as/s_3 = 82/18$ specimen (no. 3) showed no birefringence up to 120 °C but showed birefringence at 130 and 140 °C. The birefringence disappeared when the specimen was further annealed above 150 °C. In addition, on cooling process, the specimen showed the birefringence, when it was sufficiently annealed at 130 and 140 °C. However, it became nonbirefringent as the specimen was cooled down below 120 °C. These experimental evidence suggest that as/s_3=82/18 thermo-reversibly changes its optical properties, namely, it is nonbirefringent at the temperatures $T \leq 120$ °C or $T \geq 150$ °C, and birefringent at the temperatures 130 °C $\leq T \leq$ 140 °C. (iii) The specimen $as/s_3 = 85/15$ (no. 2) proved to be birefringent at temperatures between 90 and 150 °C, while nonbirefringent at $T \geq 150$ °C on both heating and cooling processes. However some hysteresis phenomena were observed in the temperature range of $T \leq 80$ °C; upon first heating of the specimen dried at 80 °C from ambient temperature, $as/s_3 = 85/15$ showed nonbirefringence, while on the cooling process from high temperature ($T \geq 150$ °C) the specimen remained birefringent within the time scale of the measurement (several hours at $T \leq 80$ °C). This hysteresis will be discussed later in section III.3.3.

III.3.2. SAXS Study for as/s_3=82/18. The temperature dependence of the SAXS profile of as/s_3=82/18 on heating and cooling processes are shown in Figure 4, parts a and b, respectively. In these figures, the higher-order peak at $q/q_m \approx 1.9$, indicative of the unidentified bicontinuous morphology as elucidated in our previous paper,[1] is marked by thick open arrows. Other higher-order peaks, which are considered to indicate a morphology other than the bicontinuous one, are marked by thin filled arrows.

Let us first discuss the heating process (see section II.2 for the thermal protocol). In Figure 4a, the profiles measured at 125 and 135 °C show the two distinct higher-order peaks at $q/q_m = \sqrt{3}$ and $q/q_m = \sqrt{4}$, respectively. These profiles are typical of hex cylinder or bcc sphere. The birefringence observed over the same temperature range (cf. section III.3.1) suggests that this morphology is hex cylinder rather than bcc sphere. At 80 and 115 °C, the profiles exhibit common features of the unidentified bicontinuous morphology having the second order peak at $q/q_m = 1.9$. This peak position does not definitely locate either at $q/q_m = \sqrt{3}$ or 2. The transmission electron micrographs (TEM) of the unidentified bicontinuous morphology is very similar to the TEM for the distorted bicontinuous morphology

shown in Figure 7b in ref 3 for the $as/s_3 = 75/25$ mixture. In fact we could not distinguish the TEMs for those two specimens by any means. Thus the TEM for the $as/s_3 = 82/18$ mixture was not repeatedly shown in this paper. The TEM clearly indicated a bicontinuous microdomain structure with some distortions in the long-range order. The distortions, which can be discerned also from the relatively broad first-order and second-order peaks compared with those from hex cylinder, made identification of its space group symmetry difficult. Thus we denoted the structure as an unidentified bicontinuous structure[1]. The unidentified structure might be either a distorted double gyroid[31–33] or a *Fddd*[34,35] structure.

At 147.5 °C, the second order peak broaden into a shoulder, and hence the lattice distortions are much larger than those at 80 and 115 °C. TEM image exhibited the distorted bicontinuous morphology.[3] Thus, the specimen is considered to undergo the OOT between bicontinuous and hex cylinder (hereafter designated as B−C OOT) twice as the temperature increased from 80 to 180 °C. The low temperature B−C OOT occurred between 115 and 125 °C from the unidentified bicontinuous structure to hex cylinder, and the high temperature "OOT" occurred between 135 and 147.5 °C from hex cylinder to the distorted bicontinuous structure with a very low degree of order. In a rigorous sense the high temperature "OOT" should be termed as OdOT (order−distorted order transition) as described earlier. This is why the quotation mark is put on OOT. Hereafter "OOT" designates the transition involving OdOT for the sake of convenience.

A similar OOT behavior was observed on the cooling process from 180 °C (Figure 4b). In the temperature range $T < 116$ °C, the shoulder at $q/q_m \approx 1.9$ typical of the unidentified bicontinuous morphology was confirmed. Above 147 °C, a very broad second-order shoulder can be observed, which does not disappear up to 180 °C. In this temperature range of $147 < T < 180$ °C, the specimen had the distorted bicontinuous structure with a very low degree of order. Judging from the clear piece of evidence for existence of hex cylinder at 125 and 135 °C on the heating process, the profiles measured at 116 and 126 °C in Figure 4b also seem to indicate hex cylinder morphology. However, on these two profiles, the second-order peak is not located exactly at $q/q_m=\sqrt{3}$ and the first-order peak is as broad as ones measured at other temperatures (i.e., 147 and 74 °C). These features may indicate a distorted hex cylinder. The reorganization of the microdomains was very slow and a 1-h waiting period before the SAXS measurement may not be sufficient enough for a full reorganization of the microdomain structure into hex cylinder.

The difference between cooling and heating processes is well reflected on the behaviors of the I_m^{-1}, σ_q^2, and D vs T^{-1}, which are shown respectively in the Figure 5a−c. During the heating process a discontinuous drop of σ_q^2 observed between 122 and 125 °C indicates that the cylindrical microdomains were organized much more regularly than that of the unidentified bicontinuous structure. During the cooling process, the transition from distorted bicontinuous to hex cyl does not attain reorganization of microdomain structures to such a level that causes the discontinuity of D observed in the heating process. However the symmetry change in the morphology brought about by this transition is perceivable from a discontinuous change in the ratio of the q-value at the second-order peak (q_{m2}) to that at first-order peak (q_{m1}) as presented in Figure 5d. The bicontinuous phase at the low temperatures is more ordered than the bicontinuous phase at the high temperatures, as clearly evidenced from the fact that the former has (i) the sharper first-order peak (i.e., smaller σ_q^2 in Figure 5b) and the more distinct second-order peak at $q/q_m = 1.9$ (Figure 4) than the latter. From this viewpoint we shall define the low temperature bicontinuous phase as an "unidentified bicontinuous" phase and the high temperature bicontinuous phase as a "distorted bicontinuous phase".

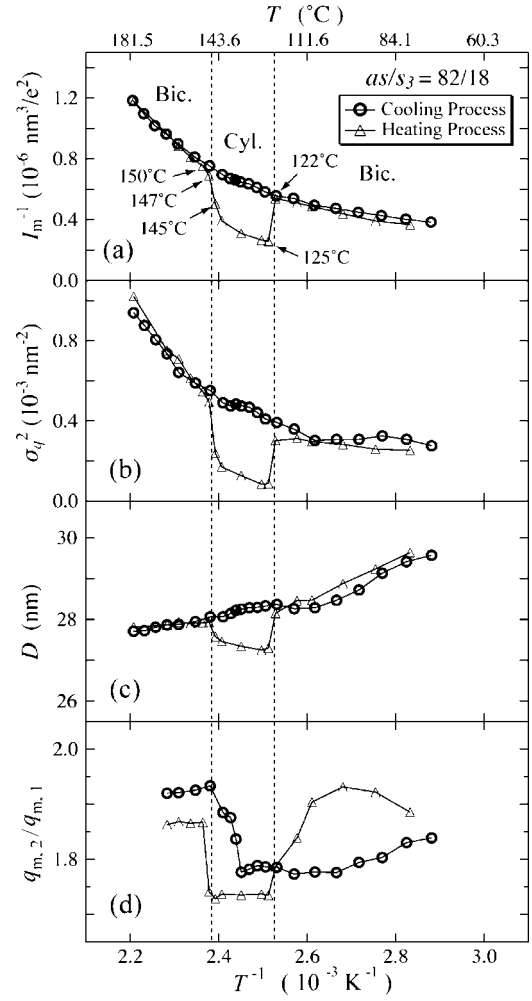

Figure 5. Temperature dependence of (a) I_m^{-1}, (b) σ_q^2, (c) D, and (d) $q_{m,2}/q_{m,1}$, the ratio of the q-value at the second-order scattering peak (designated as $q_{m,2}$) to that at the first-order scattering peak (designated as $q_{m,1}$), respectively, for $as/s_3 = 82/18$ mixture.

As a summary, this mixture $as/s_3 = 82/18$ showed a re-entrant B−C "OOT" (here, B denotes either "unidentified bicontinuous" or "distorted bicontinuous" phase, while C does hex cyl). Both the low and high temperature B−C OOTs are essentially thermoreversible, though, a large hysteresis phenomenon was observed on the cylindrical phase and the regularity of cylindrical microdomains attained during the cooling process was much worse than that during the heating process. The transition from the distorted bicontinuous structure to hex cylinder is slower than the transition from the unidentified bicontinuous structure to hex cyl.

III.3.3. Comparison between $as/s_3 = 82/18$ and $as/s_3 = 85/15$. The morphological change of $as/s_3 = 85/15$ as a function of temperature is similar to that of $as/s_3 = 82/18$. Although the scattering curves are not shown in this paper, temperature dependence of the scattering behavior of $as/s_3 = 85/15$ is described below. Upon cooling the specimen of $as/s_3 = 85/15$ from 180 to 150 °C, the specimen was in the distorted bicontinuous phase. Around 145 °C, the specimen underwent a B−C "OOT" (or OdOT). At temperatures lower than 146 °C the cylindrical structure became stable and this morphology was kept until 80 °C. The bicontinuous structure, which was clearly observed on the specimen dried at 80 °C and before the annealing at 180 °C, was only partially recovered even after

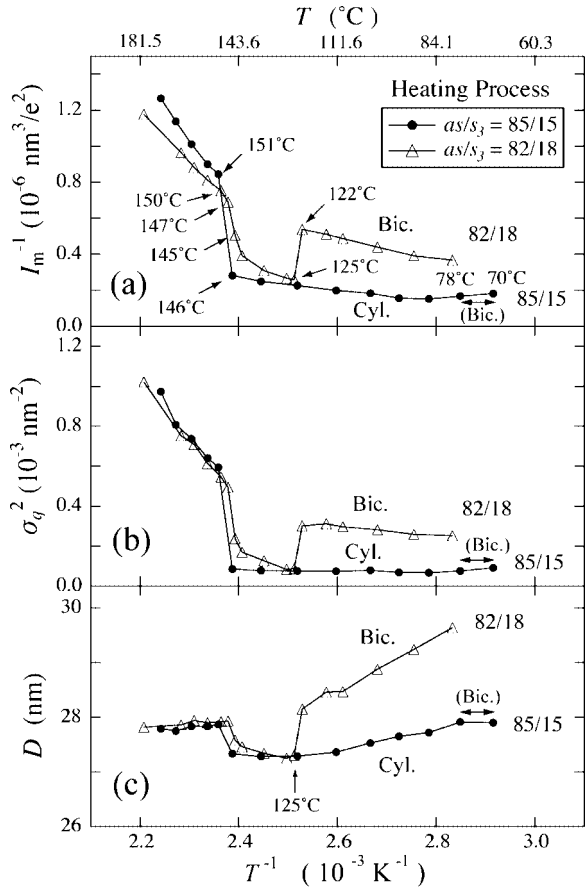

Figure 6. Comparison of the temperature dependence of the characteristic parameters of the first-order scattering peak between as/s_3 = 82/18 and 85/15: (a) I_m^{-1}, (b) σ_q^2, and (c) D, respectively. The data were obtained in the heating process.

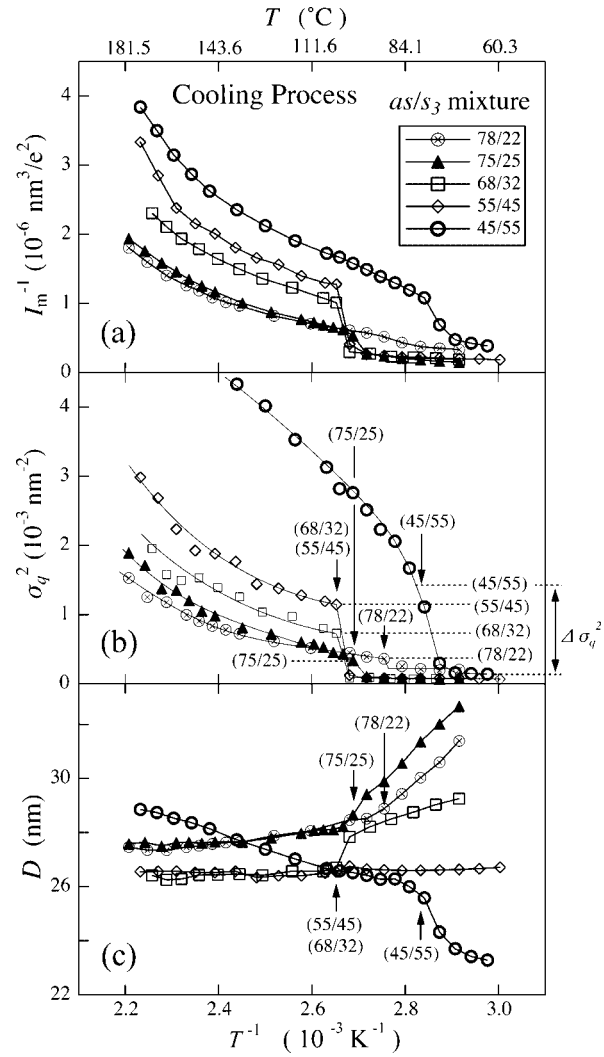

Figure 7. Comparison of the temperature dependence of the characteristic parameters of the first-order scattering peak among the as/s_3 mixtures having varying blending composition, each of which undergoes the transition between lamellae and distorted bicontinuous structure: the transition temperature for each specimen is indicated by the arrow; (a) I_m^{-1}, (b) σ_q^2 and (c) D. In part b, the amount of the change in σ_q^2 in between the onset and completion of OOT is denoted by $\Delta\sigma_q^2$, and the level of the minimum σ_q^2 of the distorted bicontinuous phase for each specimen is indicated by a broken line.

the prolonged annealing for 48 h at 75 °C and hence the birefringence of the specimen remained due to the coexistence of cylindrical domains with the distorted bicontinuous phase (cf. section III.3.1). This experimental evidence indicates that the lower temperature B−C OOT during the cooling process occurs around 75 °C. However, it is difficult to attain the completion of this transition within a limited time scale of observation, because the temperature is very close to the glass transition temperature of PS domains, where the kinetics of OOT is extremely slow. This is why we put "Bic" in parentheses in the legend of Figure 6 to be discussed immediately below. On the subsequent heating process, a well-ordered hex cylindrical phase was observed from 80 to 146 °C, and then the specimen transformed into the distorted bicontinuous phase above 151 °C.

Figure 6 compares the temperature dependence of scattering parameters I_m^{-1}, σ_q^2, and D for as/s_3 = 85/15 with that for as/s_3 = 82/18 on the heating process. In the figure, there is a temperature range (between 70 and 78 °C) marked by (Bic). This means that some bicontinuous domains did coexist in this temperature range as a consequence of the low temperature OOT at around 80 °C, as described earlier in section III.3.1 and in the beginning of this section, although the parameters of I_m^{-1}, σ_q^2, and D in the figures do not present a remarkable signature of this OOT at all.

At high temperatures the microdomain structures of both specimens as/s_3 = 85/15 and 82/18 have almost identical characteristics with respect to I_m^{-1}, σ_q^2, and D. Then at 145 ± 4 °C, both mixtures underwent the high temperature B−C "OOT" (or OdOT) as evidenced by the discontinuity of I_m^{-1}, σ_q^2, and D. The cylindrical microdomain structures of these two mixtures in the heating process (125 ≤ T(°C) ≤ 146) are also very similar with respect to the dimension (D) and the regularity (σ_q^2). The main difference between these two mixtures are seen in the thermoreversibility of the low temperature OOT (being poor for as/s_3 = 85/15 and good for as/s_3 = 82/18) and the temperature breadth for the stability of the hex cylinder (being large for as/s_3 = 85/15 and small for as/s_3 = 82/18). The latter difference is attributed to the difference in the low temperature OOT. Since the difference in composition between as/s_3 = 82/18 and 85/15 is sufficiently small, it seems natural that the behaviors of I_m^{-1}, σ_q^2, and D of these two mixtures are nearly identical above 125 °C. In contrast, the serious discrepancy between them at lower temperature seems anomalous. We will explain this anomaly from the viewpoint of the cosurfactant effect later in the discussion section (section IV.2).

III.4. Transition between Lamella and Distorted Bicontinuous. In the previous study,[3] we elucidated that two different as/s_3 mixtures, i.e., 45/55 and 75/25, having lamellar morphology at ambient temperature, underwent "OOT" (or OdOT) into the distorted bicontinuous morphology at high

temperatures (see Figure 1). Here, by adding the results obtained for three more mixtures (as/s_3 = 55/45, 68/32, and 78/22) we will advance our analysis by a step further on this transition. The lamellar-distorted bicontinuous transition is clearly captured by the abrupt changes of I_m^{-1}, σ_q^2, and D with T^{-1}, indicative of first-order phase transition as in the cases of other specimens discussed so far. Parts a−c in Figure 7 show I_m^{-1} vs T^{-1}, σ_q^2 vs T^{-1} and D vs T^{-1} for five as/s_3 mixtures undergoing the transition. Since the behaviors of I_m^{-1} vs T^{-1} are very similar with those of σ_q^2 vs T^{-1}, only σ_q^2 and D will be discussed below. Note, furthermore, that the transition exhibited nearly no hysteresis in contrast with those which undergo unidentified bicontinuous−hex cyl OOT. Therefore, only the data of the cooling process are presented in Figure 7a−c.

Concerning the discontinuity of σ_q^2 vs T^{-1}, two parameters are worthy of notice, i.e., the transition temperature shown by the arrow, and the magnitude of discontinuity, $\Delta\sigma_q^2$, which is defined in Figure 7b. The transition temperature is determined by the balance of overall composition of PS, ϕ_{PS}, and segregation power of the system (cf. section V of ref 3), and hence, it does not change monotonously with ϕ_{PS}. While $\Delta\sigma_q^2$ monotonously decreases with increase of w_{as}, the weight fraction of *as* copolymer in the mixtures. This point will be discussed in the following section (sec. IV. 1).

In Figure 7c, D vs T^{-1} curves do not always show conspicuous discontinuities at their transition temperatures shown by the arrows but surprisingly depends on the mixture composition. Generally, the average slope of D vs T^{-1} increases with the *as* content: for as/s_3 = 45/55 the slope is negative, for as/s_3 = 55/45 the slope is nearly zero; for as/s_3 = 68/32 the slope turns positive. Although some of anomalous behaviors of D were already discussed in the previous study,[3] we reconsider the behaviors based on the relation between D and chain organization of *as* and s_3 in the next section (section IV.1).

IV. Discussion

IV.1. Cosurfactant Effect on the Lamellar-Distorted Bicontinuous Transition (as/s_3 = 78/22 − 45/55). Here we shall focus our interest on the following point: why the behaviors of σ_q^2 and D vs T^{-1} are so different for different compositions of as/s_3 mixtures, or what kind of physical factors control the various behaviors of σ_q^2 and D vs T^{-1}. To clarify this problem we introduce invariant, Q, as an additional parameter which definitely characterizes the segregation state of the system

$$Q = 4\pi \int_0^\infty q^2 I(q)\, dq \sim \phi(1-\phi)(\rho_A - \rho_B)^2 \qquad (2)$$

where *I(q)* is the scattering intensity from the system comprising A and B phases (corresponding to PS and PI phases, respectively), ϕ is the volume fraction of A phase, and ρ_i (i = A and B) is the electron density of i phase. Upon increasing the segregation power from a weak segregation limit to a strong segregation limit, Q is expected to increase to reach a constant value. Figure 8 presents log Q vs T^{-1} for each blend where the transition temperature for each as/s_3 mixture is marked by an arrow. It is worth noting that the five curves on Q vs T^{-1} tend to approximately fall into a master curve when Q vs T^{-1} are reduced respectively by $Q/\phi(1-\phi)$ and $T^{-1} - T_{ODT}^{-1}$. Further details on Q as to a method of its evaluation and its physical meaning are omitted here, since they were described previously in section IV-2 in ref 3.

The mixtures of as/s_3 = 78/22 and 75/25 are considered to be nearly in the strong segregation regime below their transition temperatures, since the Q values of these specimens reach nearly a constant value with respect to T^{-1} below the transition temperatures. Whereas the mixtures of as/s_3 = 68/32, 55/45, and 45/55 are not in the strong segregation regime below their

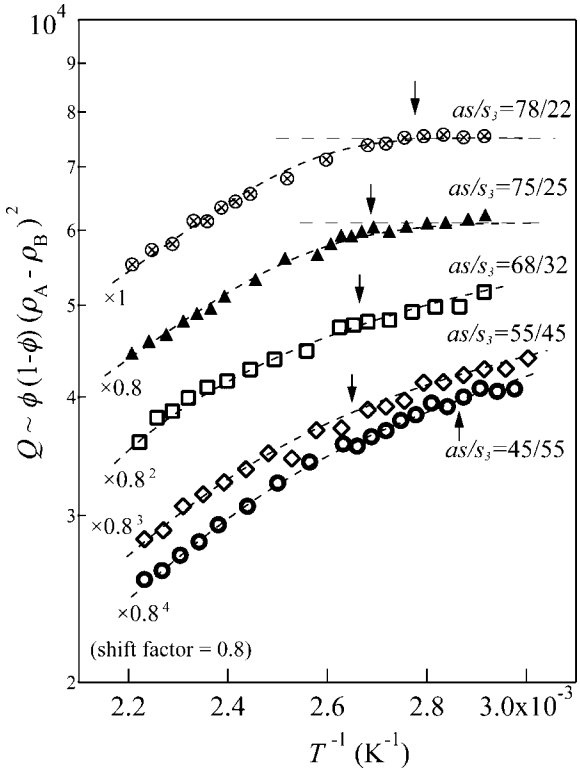

Figure 8. Plots of invariant, Q, as a function of T^{-1} for the as/s_3 mixtures, each of which undergoes the transition between lamellae and distorted bicontinuous structure at the tempeature indicated by the arrow. The vertical axis is represented in a logarithmic scale and each successive Q vs T^{-1} curve is vertically shifted by a factor of 0.8.

transition temperatures, since the Q values of these specimens seem to still increase with T^{-1}. On the contrary, the Q values of all the mixtures tend to rapidly decrease with increasing above their transition temperatures, indicating a decreasing segregation power. This implies an increasing delocalization of chemical junctions of s_3 from the interface.

The following correlations may be observed between D vs T^{-1} and Q vs T^{-1}. When the transition occurs in a strong segregation regime, D sharply increases with T^{-1} in the lamellar phase (right-hand side of the arrow in the plot shown in Figure 7c). In the cases of as/s_3 = 75/25 and 78/22, the slope of log D vs log T^{-1}(1.53) is far larger than that of neat diblock copolymers (1/3).[47] On the other hand, when the transition occurs in a rather weak segregation regime, the slope of log D vs log T^{-1} in the lamellar phase is small (as/s_3 = 68/32 and 55/45) or even negative (as/s_3 = 45/55). We have already proposed that the slope depends on the balance of the following two opposing effects:[3] (a) a decrease of D with increasing temperature due to the decrease of the segregation power and resulting relaxation of chain stretching of the copolymers whose junction points stay around interface; (b) an increase of D with increasing temperature due to the s_3 copolymers which are delocalizing from the interface and swelling the microdomains.

Let us come back to the case where the system undergoes the transition within the strong segregation regime. In that case, in the lamellar phase below the transition, chemical junctions of s_3 and *as* copolymer chains are expected to localize around the common interface, and the chemical junctions of *as* occupy the same interfacial area per junction as that occupied by the short symmetric diblock s_3.[2,3,6] Thus, for such blends, it is not surprising that a temperature decrease induces a more significant chain stretching effect than for neat SI block copolymers, which brings a sharper increase of D with T^{-1} for the blends than for the neat block copolymers.[48] We propose that the slope of D

vs T^{-1} in the lamellar phase largely depends on the degree of localization of s_3 copolymer around the microdomain interface. If s_3 copolymer chains are well localized, the slope of D vs T^{-1} is much larger than that of the neat diblock copolymer, whereas if s_3 copolymer chains are only partially localized and the fraction of the delocalized s_3 decreases with T^{-1}, the slope of D vs T^{-1} is smaller than that of neat diblock.

Let us now focus on σ_q^2 vs T^{-1}. As mentioned in section III.4, $\Delta\sigma_q^2$ simply decreases with increasing w_{as}. Since σ_q^2 is related to the regularity of the microdomain spacing, a decrease of $\Delta\sigma_q^2$ implies that a more ordered bicontinuous morphology emerges above the transition temperature. Here we can discern a correlation between $\Delta\sigma_q^2$ and the segregation state, because w_{as} affects the segregation state at the transition simply because "ODT" ("$D_{md}D_{cf}T$" or "dODT" defined in section I) temperature increases with increasing w_{as} (or decreasing w_{s_3}) as shown in Figure 1 so that the difference between the two transition temperatures ("ODT" and "OdOT" temperatures) tends to increase with w_{as}. This effect of w_{as} is also manifested from the results shown in Figure 7. The lamellar to the distorted bicontinuous transition which occurs in the strong segregation state causes the small value of $\Delta\sigma_q^2$. Another correlation can be found between Figure 7, parts b and c: the mixture, whose slope of D vs T^{-1} is larger, has a smaller $\Delta\sigma_q^2$ at the "OOT". Since most of junction points of the copolymer chains should be localized at the interfacial area in the strong segregation regime, a less distorted morphology might emerge just above the "OOT" when the "OOT" occurs in the strong segregation limit. When the "OOT" occurs in the weaker segregation limit, a greater number of delocalized s_3 copolymer chains may be generated, and they swell the microdomains above the "OOT", which may cause a more distorted bicontinuous morphology and hence a larger value of $\Delta\sigma_q^2$.

One can find another scenario as follows. As w_{as} increases, ϕ_{PS} goes away from symmetric composition and gets closer to the stability range of the bicontinuous phase. Then, the overall spontaneous curvature of the mixture becomes more favorable to form a bicontinuous phase with a long-range order, which gives a sharp scattering peak above the "OOT". Thus, both factors, ϕ_{PS} and segregation power, may explain the σ_q^2 behavior.

IV.2. Cosurfactant Effect on the B−C "OOT" (as/s_3 =82/18, 85/15). In an as/s_3 mixture having a nonlamellar morphology, the s_3 content is relatively small. Nevertheless, the small amount of s_3 can have significant effects on the microdomain structures, as illustrated in the previous sections, sections III.2 and III.3. In this section, we consider the following two effects: one is the re-entrant nature, and the other is the unique temperature dependence of D as shown in Figures 5 and 6.

The re-entrant "OOT" as clearly observed on $as/s_3 = 82/18$ (see section III.3.2) has never been reported to the best of our knowledge on neat block copolymers. The following two characteristics inherent in the as/s_3 mixtures seem to make this re-entrant transition possible. One is that at ambient temperature the localization of a chemical junction point of s_3 at the microdomain interface considerably shifts the stability limit of the morphologies with respect to ϕ_{PS} relative to that of neat block copolymers (cosurfactant effect). For instance, the composition range of $(\phi_{PS,Bic})_{as/s_3}$ (=0.225−0.24) for the bicontinuous phase in the mixture exists in the stability range of hex cylinder phase for neat diblock copolymers (cf. Figure 1). Therefore once the degree of localization of s_3 copolymer slightly decreases with T, and hence the *cosurfactant effect* itself slightly weakens, as a consequence of decreasing segregation power with T, the system will tend to recover cylindrical morphology inherent in the composition, and hence, the low temperature B−C OOT between the unidentified bicontinuous phase and hex cyl occurs. The conjecture that a small fraction of the delocalization of s_3 is sufficient for the low temperature B−C OOT will be supported in the following two paragraphs in conjunction with D vs T^{-1} in Figure 6. The high temperature B−C "OOT" is interpreted as a disordering of the ordered hex-cylinder phase into the distorted bicontinuous phase as in the case of the L-B "OOT". Here only the volume fraction of the network phase will be different between the two distorted bicontinuous phases, one from the hex-cylinder phase and the other from the lamellar phase. In both distorted bicontinuous phases there will be a large amount of s_3 delocalized from the interface as will be clarified immediately below.

The second issue is the unique temperature dependence of D. For the as/s_3=82/18 mixture there are two temperature regions of bicontinuous phase, one is above 150 °C and the other is below 122 °C. Although the two phases appear to be similar on their SAXS profiles or TEM images, there is a large difference in their D vs T^{-1} behaviors. Above 150 °C, D hardly depends on T^{-1}, suggesting that the two opposing effects work on D as discussed in section IV.1. However, below 122 °C, D clearly increases with T^{-1}, implying that the chemical junction points of the s_3 chains should be well segregated around the microdomain interface.

Furthermore, the comparison of D vs T^{-1} behavior of as/s_3 =82/18 with that of 85/15 (cf. Figure 6) is worth noting to understand the strength of the *cosurfactant effect* at low and high temperatures. One should recall the following three points: (i) the difference of s_3 content between the two mixtures is only 3% in weight fraction; (ii) at high temperatures ($T \geq 125$ °C), the behavior of D vs T^{-1} (as well as morphology) is almost identical between the two mixtures; (iii) however, at low temperatures (T ≤ 122 °C), the behavior of D vs T^{-1} becomes considerably different. Those experimental evidences suggest that the impact of the difference in s_3 content between the two mixtures (only 3% in weight fraction) upon D vs T^{-1} behavior became more and more significant with lowering temperature, indicating increasing significance of *cosurfactant effect* with lowering T.

IV.3. Phase Diagram. The morphological data newly obtained for the as/s_3 mixtures are put together with those previously reported[3] and a phase diagram is constructed in the parameter space of ϕ_{PS} and T as shown in the $\phi_{PS}-T$ plane in Figure 9. The $\phi_{PS}-T$ phase diagram is further combined with the $\phi_{PS}-r$ phase diagram, which was presented in the first paper of this series of works.[1] The resulting three-dimensional phase diagram is shown in Figure 9, where the three coordinates (x, y, and z) correspond to ϕ_{PS}, r, and T, respectively. The figure includes the composition range for various morphologies in the neat SI block copolymer as a reference: bcc sphere, hex cylinder, ordered bicontinuous structure, and lamella that are denoted respectively as S, Cyl, Bic, and Lam. In this phase diagram the both ends of the ϕ_{PS}-axis are then corresponding to neat *as* and neat s_i (i = 1, 2, and 3) copolymers, respectively; neat *as* copolymer, having the smallest ϕ_{PS} (= 0.185) and bcc sphere, locates on the left-hand edge, whereas neat s_i (i = 1, 2 and 3) copolymers, which are nearly symmetric ($\phi_{PS} = 0.455 - 0.49$) and have lamellar morphology (s_1, s_2) or a disordered state (s_3), are found on the right-hand edge. It should be noted here that although a three-dimensional phase diagram is constructed, the $\phi_{PS}-T$ phase diagram was investigated only for the as/s_3 (r = 4.40) mixtures and those for as/s_2 (r = 3.63) mixtures and as/s_1 (r = 2.87) mixtures were left unexplored in this series of works.[49]

The following six morphologies were observed in the three-dimensional phase diagram: (i) bcc-sphere denoted by S; (ii) hex cylinder denoted by Cyl; (iii) unidentified bicontinuous

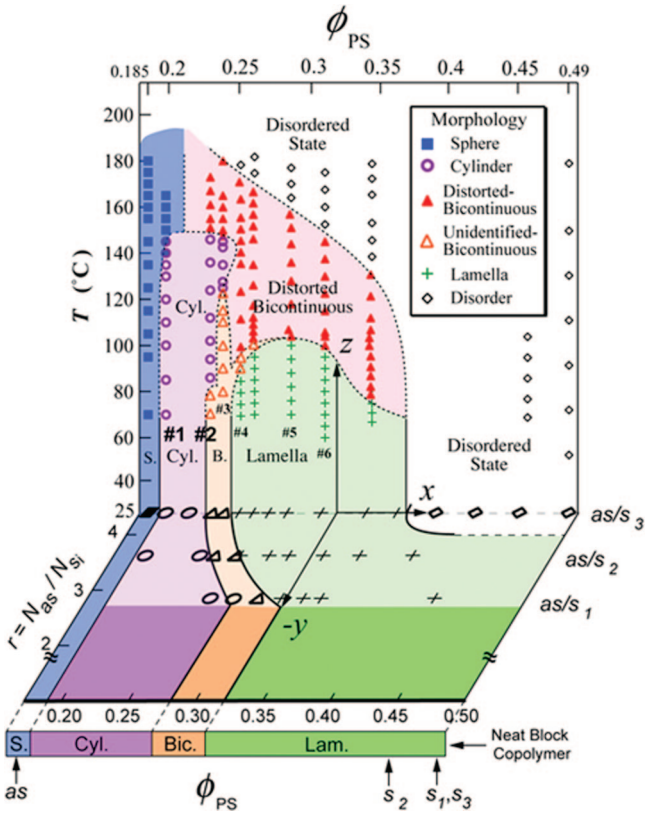

Figure 9. Three-dimensional phase diagram of the as/s_i ($i = 1$, 2, and 3) mixture system in the parameter space of the overall volume fraction of the PS block chains, ϕ_{PS}, the ratio of the total chain length of long copolmer (N_{as}) to that of short copolymer (N_{si}), r, and temperature, T.

phase denoted by B or Bic; (iv) distorted bicontinuous phase; (v) lamella; (vi) disordered phase.

The key concept underlying in the phase diagram is the *cosurfactant effect*. The most conspicuous role of the cosurfactant effect on this phase diagram is seen in an enlargement of the stability limit of the lamellar morphology.[1] This effect is clearly observed in the $\phi_{PS}-r$ plane. The composition (ϕ_{PS}) range for the lamellar phase expands with increasing r above ca. 2.8, while the composition range is the same as that for the neat block copolymer for $r \leq 2.8$. The large expansion of the lamellar phase involves a large contraction of the hex cylinder phase and a slight contraction of the bicontinuous phase. The expanded lamellar phase keeps its stability up to 100 °C along the temperature axis. This temperature limit is expected to increase with decreasing r, though the composition range for the lamellar morphology becomes narrower. Upon further increase in T, the lamellar phase is first transformed into the distorted bicontinuous phase and subsequently into disordered phase. The extended distorted bicontinuous phase and the temperature-induced re-entrant unidentified bicontinuous-cylinder-distorted bicontinuous "OOT" (OdOT) also are believed to arise from the cosurfactant effects.

The comparison of $as/s_3 = 85/15$ (no. 2) with $as/s_3 = 97/03$ (no. 1) is of interest in regard to their morphological changes at high temperatures. Over the temperature range between 85 and 140 °C, both mixtures have hex cylinder, while above 150 °C, the former transforms into the distorted bicontinuous phase but the latter transforms into the bcc-sphere phase. This difference is another striking illustration of the richness of possibilities concerning morphology controls offered by the cosurfactant effect.

V. Concluding Remarks

The characteristics of microphase-separated structure for a series of binary mixtures composed of polystyrene-*block*-polyisoprene diblock copolymers have been investigated in this series of study. This is the first systematic experimental work, which focuses on the morphology control based on the principles of the *cosurfactant effect*. A careful choice of a symmetric short copolymer and an asymmetric long copolymer makes it possible that the two copolymers are mixed with each other at molecular level and their chemical junctions share a common interface without involving macrophase separation. As summarized in the phase diagram in the parameter space (T, r, and ϕ_{PS} or w_{as}) shown in Figure 9, the following novel features, which have never been observed in neat block copolymers, were obtained: (1) in the strong segregation regime, lamellar morphology is particularly stabilized, extending its stability limit in the parameter space of r and w_{as} (or ϕ_{PS}), whereas (2) in the weak segregation regime the distorted bicontinuous morphology is particularly stabilized; (3) a novel, the unidentified bicontinuous morphology emerges at a certain composition range; (4) a novel re-entrant type temperature-induced "order-order" transition, which involves the transition from the unidentified bicontinuous phase (probably the distorted double gyroid or *Fddd* orthorhombic phase) to hex cylinder and that from hex cylinder to the distorted bicontinuous phase, was observed at a particular blend composition. Complementarily to the feature in ref 1, the stability range of the hex-cylinder was naturally suppressed.

Two key features make the system investigated here of particular interest. Those are the *cosurfactant effect* primarily due to (i) the large difference between the molecular characteristics of the two diblocks and (ii) the short symmetric diblock s_3 which gives the possibility for the chemical junctions to migrate away from the interface over the experimentally accessible temperature range. The richness of the phase diagram of such binary blends, especially the various kinds of phase transitions observed renew the interest on these systems.

References and Notes

(1) Court, F.; Hashimoto, T. *Macromolecules* **2001**, *34*, 2536.
(2) Court, F.; Hashimoto, T. *Macromolecules* **2002**, *35*, 2566.
(3) Court, F.; Yamaguchi, D.; Hashimoto, T. *Macromolecules* **2006**, *39*, 2596–2605.
(4) Lin, E. K.; Gast, A. P.; Shi, A.-C.; Noolandi, J.; Smith, S. D. *Macromolecules* **1996**, *29*, 5920–5925.
(5) Hasegawa, H.; Hashimoto, T. In *Comprehensive Polymer Science, Second Supplement*, Aggarwal, S. R., Russo, S., Vol. Eds.; Pergamon: Oxford, U.K., 1996; Chapter 14, pp 497−539.
(6) (a) Birshtein, T. M.; Liatskaya, Y. V.; Zhulina, E. B. *Polymer* **1990**, *31*, 2185. (b) Zhulina, E. B.; Birshtein, T. M. *Polymer* **1991**, *32*, 1299. (c) Zhulina, E. B.; Lyatskaya, Y. V.; Birshtein, T. M. *Polymer* **1992**, *33*, 332. (d) Lyatskaya, J. V.; Zhulina, E. B.; Birshtein, T. M. *Polymer* **1992**, *33*, 343. (e) Birshtein, T. M.; Lyatskaya, Y. V.; Zhulina, E. B. *Polymer* **1992**, *33*, 2750.
(7) (a) Shi, A.-C.; Noolandi, J. *Macromolecules* **1994**, *27*, 2936. (b) Shi, A.-C.; Noolandi, J.; Hoffmann, H. *Macromolecules* **1994**, *27*, 6661. (c) Shi, A.-C.; Noolandi, J. *Macromolecules* **1995**, *28*, 3103. (d) Cooke, D. M.; Shi, A.-C. *Macromolecules* **2006**, *39*, 6661.
(8) (a) Milner, S. T.; Witten, T. A.; Cates, M. E. *Macromolecules* **1988**, *21*, 2610–2619. (b) Milner, S. T.; Witten, T. A.; Cates, M. E. *Macromolecules* **1989**, *22*, 853–861.
(9) (a) Yamaguchi, D.; Hashimoto, T. *Macromolecules* **2001**, *34*, 6495–6505. (b) Yamaguchi, D.; Hasegawa, H.; Hashimoto, T. *Macromolecules* **2001**, *34*, 6506–6518.
(10) Hashimoto, T.; Yamaguchi, D.; Court, F. *Macromol. Symp.* **2003**, *195*, 191–200.
(11) Hashimoto, T.; Yamauchi, K.; Yamaguchi, D.; Hasegawa, H. *Macromol. Symp.* **2003**, *201*, 65–75.
(12) Chen, F.; Kondo, Y.; Hashimoto, T. *Macromolecules* **2007**, *40*, 3714–3723.
(13) Fredrickson, G. H.; Helfand, E. *J. Chem. Phys.* **1987**, *87*, 697.

(14) Hashimoto, T.; Koga, T.; Koga, T.; Sakamoto, N. In *The Physics of Complex Liquids*; Yonezawa, F., Tsuji, K., Kaji, K., Doi, M., Fujiwara, T., Eds.; World Scientific: Singapore, 1998; pp 291−308.
(15) Sakamoto, N.; Hashimoto, T. *Macromolecules* **1998**, *31*, 3815.
(16) Leibler, L. *Macromolecules* **1980**, *13*, 1602.
(17) Fredrickson, G. H.; Binder, K. *J. Chem. Phys.* **1989**, *91*, 7265.
(18) Hohenberg, G. H.; Swift, J. B. *Phys. Rev. E* **1995**, *52*, 1828.
(19) Bates, F. S.; Rosedale, J. H.; Fredrickson, G. H. *J. Chem. Phys.* **1990**, *92*, 6255.
(20) Stühn, B.; Mutter, R.; Albrecht, T. *Europhys. Lett.* **1992**, *18*, 427.
(21) Wolf, T.; Burger, C.; Ruland, W. *Macromolecules* **1993**, *26*, 1707.
(22) Hashimoto, T.; Ogawa, T.; Han, C. D. *J. Phys. Soc. Jpn.* **1994**, *63*, 2206.
(23) Floudas, G.; Pakula, T.; Fischer, E. W.; Hadjichristidis, N.; Pispas, S. *Acta Polym.* **1994**, *45*, 176.
(24) Hashimoto, T.; Takenaka, M.; Izumitani, T. *Polym. Commu.* **1989**, *30*, 45.
(25) Takenaka, M.; Izumitani, T.; Hashimoto, T. *J. Chem. Phys.* **1990**, *92*, 4566.
(26) Jinnai, H.; Hashimoto, T.; Lee, D.; Chen, S. H. *Macromolecules* **1997**, *30*, 130.
(27) Hashimoto, T.; Koga, T.; Jinnai, H.; Nishikawa, Y. *IL Nuovo Cimento* **1998**, *20*, 1947.
(28) Hashimoto, T.; Jinnai, H.; Nishikawa, Y.; Koga, T. *Macromol. Symp.* **2002**, *190*, 9.
(29) Hashimoto, T. *J. Polym. Sci., Part B: Polym. Phys.* **2004**, *42*, 3027.
(30) Sakurai, S.; Kawada, H.; Hashimoto, T.; Fetters, L. J. *Macromolecules* **1993**, *26*, 5796–5802.
(31) Hajduk, D. A.; Harper, P. E.; Gruner, S. M.; Honeker, C. C.; Kim, G.; Thomas, E. L.; Fetters, L. J. *Macromolecules* **1994**, *27*, 4063–4075.
(32) Förster, S.; Khandpur, A. K.; Zhao, J.; Bates, F. S.; Hamley, I. W.; Ryan, A. J.; Bras, W. *Macromolecules* **1994**, *27*, 6922–6935.
(33) Khandpur, A. K.; Förster, S.; Bates, F. S.; Hamley, I. W.; Ryan, A. J.; Bras, W.; Almdal, K.; Mortensen, K. *Macromolecules* **1995**, *28*, 8796–8806.
(34) (a) Tyler, C. A.; Morse, D. C. *Phys. Rev. Lett.* **2005**, *94*, 208302. (b) Ranjan, A.; Morse, D. C. *Phys. Rev. E* **2006**, *74*, 011803.
(35) Takenaka, M.; Wakada, T.; Akasaka, S.; Nishitsuji, S.; Saijo, K.; Shimizu, H.; Kim, M. I.; Hasegawa, H. *Macromolecules* **2007**, *40*, 4399–4402.
(36) Schulz, M. F.; Bates, F. S. *Phys. Rev. Lett.* **1994**, *73*, 86–89.
(37) Sakurai, S.; Irie, H.; Umeda, H.; Nomura, S.; Lee, H. H.; Kim, J. K. *Macromolecules* **1998**, *31*, 336–343.
(38) Zhao, J.; Majumdar, B.; Schulz, M. F.; Bates, F. S.; Almdal, K.; Mortensen, K.; Hajdak, D. A.; Gruner, S. M. *Macromolecules* **1996**, *29*, 1204–1215.
(39) Fujimura, M.; Hashimoto, T.; Kawai, H. *Mem. Fac. Eng., Kyoto Univ.* **1981**, *43* (2), 224.
(40) Hashimoto, T.; Suehiro, S.; Shibayama, M.; Saijo, K.; Kawai, H. *Polym. J.* **1981**, *13*, 501.
(41) Suehiro, S.; Saijo, K.; Ohta, Y.; Hashimoto, T. *Anal. Chim. Acta.* **1986**, *189*, 41.
(42) Guinier, A.; Fournet, G. *Small-Angle Scattering of X-rays*; J. Wiley& Sons: New York, 1955.
(43) Brumberg, H., Ed. *Small-Angle X-ray Scattering*; Gordon & Breach: New York, 1965.
(44) Balta-Calleja, F. J.; Vonk, C. G. *X-ray Scattering of Synthetic Polymers*; Elsevier: Amsterdam, 1989.
(45) Hendricks, R. W. *J. Appl. Crystallogr.* **1972**, *5*, 315.
(46) Sakamoto, N.; Hashimoto, T. *Macromolecules* **1995**, *28*, 6825.
(47) Hashimoto, T.; Shibayama, M.; Kawai, H. *Macromolecules* **1983**, *16*, 1093.
(48) In the blends the chain stretching of *as* and s_3 is considered to couple each other in order to satisfy incompressibility of the two layers in lamellae (one composed of both short and long chains and the other composed of long chains only[6]).
(49) Missing parts of the $\phi_{PS}-T$ phase diagrams for as/s_2 and as/s_1 mixtures are mainly owing to the fact that observations of the whole temperature behavior of the as/s_i ($i = 1, 2$) specimens, including "ODT", were difficult, because the T_{ODT}s of as/s_i ($i = 1, 2$) exist above 200 °C, so that the T_{ODT} is no longer correctly determined due to the thermal degradation of the specimen.

MA800102A